Separation phenomena in the tritium source and numerical simulations of turbo-molecular pumps

Felix Sharipov and Denize Kalempa
Departamento de Física, Universidade Federal do Paraná
Caixa Postal 19044, Curitiba, 81531-990, Brazil

September 28, 2005

Nomenclature

Notation	quantity	Unit
b	width of blades	m
$C(x)$	local concentration	
C_{col}	column concentration	
C_{in}	injection concentration	
h	distance between blades	m
J_α	dimensionless throughput of species α	
L	source tube length	m
m	molecular mass	atom unit
m_α	molecular mass of species α	atom unit
N	column density of mixture	$1/\mathrm{cm}^2$
N_α	column density of species α	$1/\mathrm{cm}^2$
N_b	number of blades	
N_g	number of generated particles	
N_r	number of rotors	
N_s	number of stators	
$n(x)$	local number density	m^{-3}
n_α	number density of species α	m^{-3}
n_{in}	number density in injection chamber	m^{-3}
P_{in}	pressure of mixture in injection chamber	bar
$P_{\alpha,in}$	pressure of species α in injection chamber	bar
q	throughput of mixture	mbar l/s
q_α	throughput of species α	mbar l/s

Notation	quantity	Unit
R	tube radius	m
R_{ex}	external radius of rotor/stator	m
R_{in}	internal radius of rotor/stator	m
R_{ms}	mean square radius of rotor/stator	m
R_g	gaseous constant	8.31441×10^3J/(kilomole K)
S	pumping speed	l/s
T	temperature of gas	K
T_p	temperature of pump	K
U	speed of rotors	m/s
v_0	characteristic molecular speed	m/s
v_m	most probable molecular speed	m/s
W	transmission probability	
x	longitudinal coordinate	m
α_i	inclinations of ith blade	
δ	rarefaction parameter	
$\Lambda_{\alpha\beta}$	kinetic coefficients	
μ	viscosity	Pa s
ω	rotation speed	s^{-1}

1 Introduction

In the previous works [1, 2], the results of numerical calculations of tritium flow from the buffer vessel up to the first vacuum system were reported. Two values of the tritium source temperature were considered, i.e. 27 K and 30 K. It was found that to maintain the column density about 5×10^{17} 1/cm^2 the injection pressure must be equal to P_{in}=3.006×10^{-3} mbar and P_{in}=3.350×10^{-3} at T=27 K and T=30 K, respectively. The corresponding throughput must be equal to q =1.853 mbar l/s and q =1.892 mbar l/s, respectively. The same calculations were carried out for the temperature T =120 K too. In these calculations it was assumed the gas to be single, i.e. no impurities are available in tritium. However, the tritium gas is never pure but some other isotope gases, like D_2, H_2, DT, HT, DH are present. Since a lighter gas has a higher thermal speed it flows faster in the transition and free molecular regimes, i.e. the separation phenomenon arises, which leads to a non-uniform concentration along the source. It is expected that in the mixture H_2 - T_2 the separation phenomenon is

sufficiently weak to be neglected. For the mixture Kr - T_2 such a phenomenon can be strong because of the large difference in the molecular masses. As a result it can affect significantly the distribution of krypton along the source.

The first aim of the present work is to calculate the separation phenomena in the source. The results of these calculations will allow us to provide more exact information about the column density of tritium and about its distribution along the source. Moreover, the krypton distribution along the source will be calculated taking into account the separation phenomenon.

Usually, a manufacturer of pumps provides the performance characteristics in accordance with the international standard [3], i.e. the pumping speed must be measured for nitrogen at T=293 K. However, the tritium source will be maintained at T=30 K. Such a difference in the temperature can significantly change the pump performance. Moreover, a performance of turbo-molecular pump is lower for a light gas than that for a heavy one. Such a difference leads to an increasing of the concentration of a light species in the vacuum systems compared with the concentration in the injection point.

The second aim of the project is to elaborate a 2D numerical model of turbo-molecular pump, which will allow us to predict the pumping speed for tritium at the low temperature using the characteristics measured for nitrogen at the room temperature.

2 Separation phenomenon

2.1 General remarks

As is known when a gaseous mixture flows through a long tube [4] or channel [5, 6, 7] then every species has its own speed. The speed difference causes the so-called separation phenomenon, i.e. the mixture concentration is not constant along the tube and the concentration in the down flow container is not equal to that in the up flow one. The magnitude of the phenomenon depends on the molecular mass ratio. It becomes significant for a mixture with a high mass ratio.

To calculate the separation phenomenon the methodology described in Ref.[8] was used.

The calculations are carried out in terms of dimensionless throughput defined as

$$J_\alpha = \frac{L}{\pi R^3 P_{in}} \left(\frac{T}{273.15}\right) \left[\frac{m(C_{in})}{2R_g T}\right]^{1/2} q_\alpha, \tag{1}$$

where T is the gas temperature, L is the source length, R is the source radius, P_{in} is the injection pressure of the mixture, R_g is the gaseous constant, q_α is the throughput of species α referred to the temperature $T = 273.15$K, and $m(C_{in})$ is the mean molecular mass of the mixture given as

$$m(C) = Cm_1 + (1 - C)m_2, \tag{2}$$

C is the molar concentration

$$C = \frac{n_1}{n_1 + n_2}, \tag{3}$$

m_α is the molecular mass of species α, n_α is the number density of species α, C_{in} means the concentration in the injection chamber.

The main idea to calculate the separation phenomenon is as follows. The dimensionless throughput J_α is proportional to the density gradients of both species, i.e.

$$J_\alpha = \frac{n}{n_{in}} \left[\frac{m(C_{in})}{m(C)}\right]^{1/2} \sum_{\beta=1}^{2} \Lambda_{\alpha\beta} \frac{R}{n_\beta} \frac{\mathrm{d}n_\beta}{\mathrm{d}x}, \qquad \alpha = 1, 2, \tag{4}$$

where x is longitudinal coordinate, $\Lambda_{\alpha\beta}(C, \delta)$ are the kinetic coefficients depending on the local molar concentration C and local rarefaction parameter δ defined as

$$\delta = \frac{PR}{\mu v_0}. \tag{5}$$

Here P is the local pressure of mixture, μ is its viscosity and v_0 is the characteristic molecular velocity of mixture given as

$$v_0 = \left[\frac{2R_g T}{m(C)}\right]^{1/2}. \tag{6}$$

Eq.(4) is subject to the following boundary conditions

$$n_1 = C_{in} n_{in} \quad \text{and} \quad n_2 = (1 - C_{in})\, n_{in} \quad \text{at} \quad x = 0, \tag{7}$$

$$n_1 = 0 \quad \text{and} \quad n_2 = 0 \quad \text{at} \quad x = L/2. \tag{8}$$

First, the kinetic coefficients $\Lambda_{\alpha\beta}$ are calculated by the method given in Ref.[4] in the specified ranges of the gas rarefaction δ and molar concentration C. The McCormack kinetic equation [9] was employed. This stage took a long CPU time, since the number of values of δ and C must be sufficiently large to interpolate the functions $\Lambda_{\alpha\beta} = \Lambda_{\alpha\beta}(\delta, C)$ with a satisfactory precision. Then, the system (4) is solved numerically by the finite difference method. During these calculations the throughput J_α is fitted to satisfy the boundary conditions (7) and (8).

When the density distributions n_1 and n_2 are known the column densities are calculated as

$$N_\alpha = \int_{-L/2}^{L/2} n_\alpha(x)\,\mathrm{d}x, \qquad \alpha = 1, 2. \tag{9}$$

The column concentration can be calculated as

$$C_{col} = \frac{N_1}{N_1 + N_2}. \tag{10}$$

Besides of the density distributions the solution of Eq.(4) provides the throughput q_α for both species.

2.2 Separation phenomenon in mixture H_2 - T_2

In this section we consider a mixture of H_2 and T_2 assuming the molar concentration of the first species to be equal to 5% in the injection chamber. Our aim is to calculate the density distributions n_α, column densities N_α, column concentration C_{col} and throughput of both H_2 and T_2 under the conditions given in Table 1. The injection pressure P_{in} was calculated in the previous works [1, 2] considering tritium as a single gas for two values of the temperature $T = 27$ K and $T = 30$ K. In the present work both values of the temperature are considered.

For this purpose the kinetic coefficients $\Lambda_{\alpha\beta}$ were calculated for the molecular mass ratio $m_1/m_2 = 1/3$ and molecular diameter ratio $d_1/d_2 = 0.9369$, which was calculated from the viscosities of H_2 and T_2. 27 values of the rarefaction parameter δ were considered in the range from 0 to 25. The molar concentration C was varied from 0.05 to 0.02 considering 16 values. Totally, 432 combinations of different values of δ and C were calculated.

The results on the density distribution are given in Tables 2 and 3 for the temperatures $T = 27$ K and $T = 30$ K, respectively. The second columns in both Tables represent the

Table 1: Input data for the mixture H_2 - T_2

quantity	notation	unity	T =27 K	T =30 K
Injection pressure of mixture	P_{in}	μbar	3.006	3.350
Injection pressure of H_2	$P_{1,in}$	μbar	0.150	0.168
Injection pressure of T_2	$P_{2,in}$	μbar	2.856	3.182
Injection gas rarefaction	δ_{in}		22.7	21.6
Injection concentration of H_2	C_{in}		0.05	0.05

Table 2: Density and concentration distributions along the source for the mixture H_2-T_2 at $T = 27$ K

	single gas	mixture		
	Ref.[2]	H_2	T_2	
x(m)	$n(x)/n_{in}$	$n_1(x)/n_{1,in}$	$n_2(x)/n_{2,in}$	$C(x)$
0.0	1.0000	1.0000	1.0000	0.0500
0.50	0.9400	0.9384	0.9401	0.0499
1.00	0.8768	0.8742	0.8768	0.0499
1.50	0.8096	0.8057	0.8094	0.0498
2.00	0.7376	0.7324	0.7373	0.0497
2.50	0.6595	0.6529	0.6591	0.0496
3.00	0.5736	0.5655	0.5729	0.0494
3.50	0.4770	0.4672	0.4758	0.0491
4.00	0.3642	0.3510	0.3623	0.0485
4.50	0.2225	0.2029	0.2195	0.0464
4.70	0.1504	0.1273	0.1472	0.0435
4.90	0.0596	0.0400	0.0556	0.0365
5.00	0.0000	0.0000	0.0000	0.0297

results obtained previously [1, 2] considering T_2 as a single gas. The third columns provide the relative density of hydrogen, the same quantity for T_2 is given in the fourth columns and the local concentration C is shown in the fifth columns. It can be seen that the concentration of hydrogen decreases along the tube from 0.05 to 0.03. However, its presence does not affect the tritium distribution significantly. The density distributions at $T = 30$ K are also shown in Fig.1, where one can see that they are close to each other and to that obtained for a single gas.

The integral characteristics such as throughput of every species and the column densities are given in Table 4. The throughput of the mixture is 3% higher that calculated for a single gas in Ref.[1]. The column densities of H_2 and T_2 and the column concentrations are exactly

Table 3: Density and concentration distributions along the source for the mixture H_2-T_2 at $T = 30$ K

	single gas	mixture		
	Ref.[1]	H_2	T_2	
x(m)	$n(x)/n_{in}$	$n_1(x)/n_{1,in}$	$n_2(x)/n_{2,in}$	$C(x)$
0.00	1.0000	1.0000	1.0000	0.0500
0.50	0.9401	0.9396	0.9396	0.0500
1.00	0.8768	0.8746	0.8759	0.0499
1.50	0.8096	0.8056	0.8081	0.0498
2.00	0.7376	0.7316	0.7356	0.0497
2.50	0.6596	0.6516	0.6569	0.0496
3.00	0.5738	0.5636	0.5703	0.0494
3.50	0.4772	0.4644	0.4728	0.0492
4.00	0.3643	0.3472	0.3588	0.0485
4.50	0.2227	0.1984	0.2161	0.0461
4.70	0.1506	0.1232	0.1441	0.0431
4.90	0.0597	0.0383	0.0537	0.0362
5.00	0.0000	0.0000	0.0000	0.0297

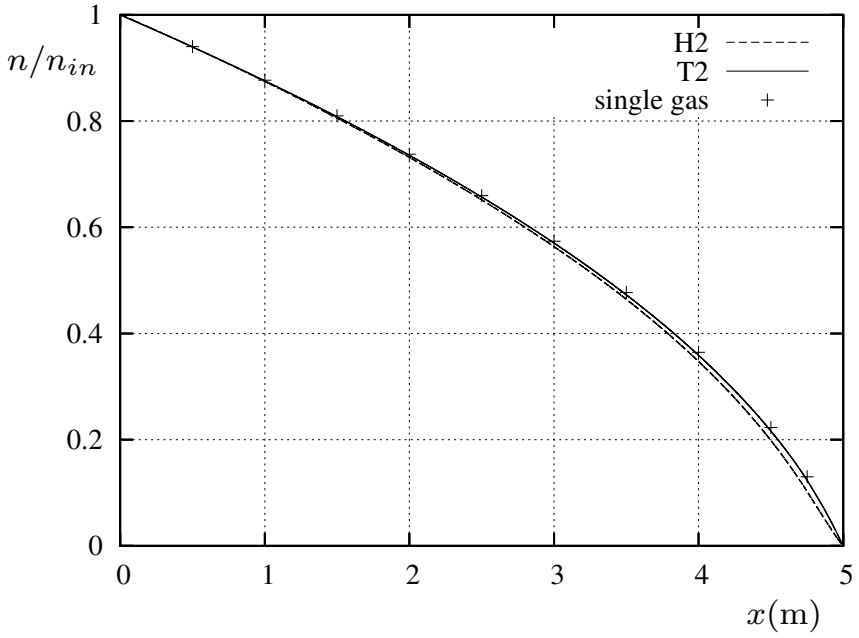

Figure 1: Density distributions of H_2 and T_2 along the source at T =30 K

Table 4: Calculated data for the mixture H_2-T_2

quantity	notation	unity	T=27 K	T=30 K
Throughput of single gas [1, 2]	q	mbar l/s	1.853	1.892
Throughput of mixture	q	mbar l/s	1.906	1.946
Throughput of H_2	q_1	mbar l/s	0.096	0.098
Throughput of T_2	q_2	mbar l/s	1.810	1.848
Column density of single gas [1, 2]	N	$10^{17}/\mathrm{cm}^2$	5.00	5.00
Column density of mixture	N	$10^{17}/\mathrm{cm}^2$	4.97	4.97
Column density of H_2	N_1	$10^{17}/\mathrm{cm}^2$	0.24	0.24
Column density of T_2	N_2	$10^{17}/\mathrm{cm}^2$	4.73	4.73
Column concentration	C_{col}		0.0494	0.0494

the same for the two different values of the temperature. Comparing these quantities with those obtained for a single gas it can be seen that the density of T_2 is 5.4% lower than that for a pure tritium, i.e., this difference is very close to the hydrogen concentration in the injection point. The column concentration C_{col} is very close to the injection concentration C_{in}.

Thus, we may conclude that the separation phenomenon for the mixture H_2-T_2 is negligible. Here, we considered an extreme situation, i.e. the maximum concentration of the impurity and its lightest component, i.e. hydrogen. Really, the concentration of the impurity is smaller and the other components, e.g. D_2, have their molecular mass closer to that of T_2. Thus, in practice the separation phenomenon will be weaker than that calculated here.

2.3 Separation phenomenon for mixture Kr - T_2

In this section a flow of the mixture Kr - T_2 is considered assuming the molar concentration of the first species to be small in the injection chamber, i.e. $C_{in} \ll 1$. We are going to calculate the density distribution of both Kr and T_2 under the conditions given in Table 5.

Since the concentration of Kr is very small we assume that it does not affect the flow of tritium, while the concentration of Kr in every cross section of the source $C(x)$ is proportional to the injection concentration C_{in}. Thus, in this section the data on the relative concentration $C(x)/C_{in}$ will be provided, which are valid for any values of C_{in} under the condition $C_{in} \ll 1$.

The kinetic coefficients $\Lambda_{\alpha\beta}$ were calculated for the molecular mass ratio $m_1/m_2 = 13.89$ and molecular diameter ratio $d_1/d_2 = 1.822$, which was calculated from the viscosities of

Table 5: Input data for the mixture Kr-T_2

Temperature	$T = 120$K
Injection pressure of mixture	P_{in}=13.80 μbar
Injection pressure of Kr	$P_{1,in}$=13.80$\times 10^{-3}$ μbar
Injection pressure of T_2	$P_{2,in}$=13.79 μmar
Injection gas rarefaction	$\delta_{in} = 13.8$

Table 6: Density and concentration distributions along the source for the mixture Kr - T_2

	T_2	Kr
x(m)	$n(x)/n_{in}$	$C(x)/C_{in}$
0.00	1.000	1.00
0.50	0.940	1.01
1.00	0.877	1.02
1.50	0.810	1.02
2.00	0.738	1.03
2.50	0.659	1.05
3.00	0.574	1.07
3.50	0.477	1.10
4.00	0.364	1.18
4.50	0.225	1.43
4.70	0.150	1.75
4.90	0.060	2.61
5.00	0.000	3.62

Kr and T_2. The rarefaction parameter δ was varied from 0 to 14 considering 28 values. The molar concentration C was varied from 0.0001 to 0.01 considering 12 values. Totally, 336 combinations of δ and C were calculated. A comparison of the results corresponding to $C_{in} = 10^{-3}$ and those for $C_{in} = 10^{-4}$ showed that the concentration in every cross section is proportional to C_{in}.

The results on the density and concentration distributions are given in Table 6. The second column represents the results obtained previously [2] considering a single gas T_2. The third columns provides the relative concentration of krypton. It can be seen that the concentration of krypton increases significantly along the tube. The concentration distributions is also shown in Fig.2.

The integral characteristics such as throughput of every species and the column densities are given in Table 7. The column concentration of Kr is 6% higher than its value in the

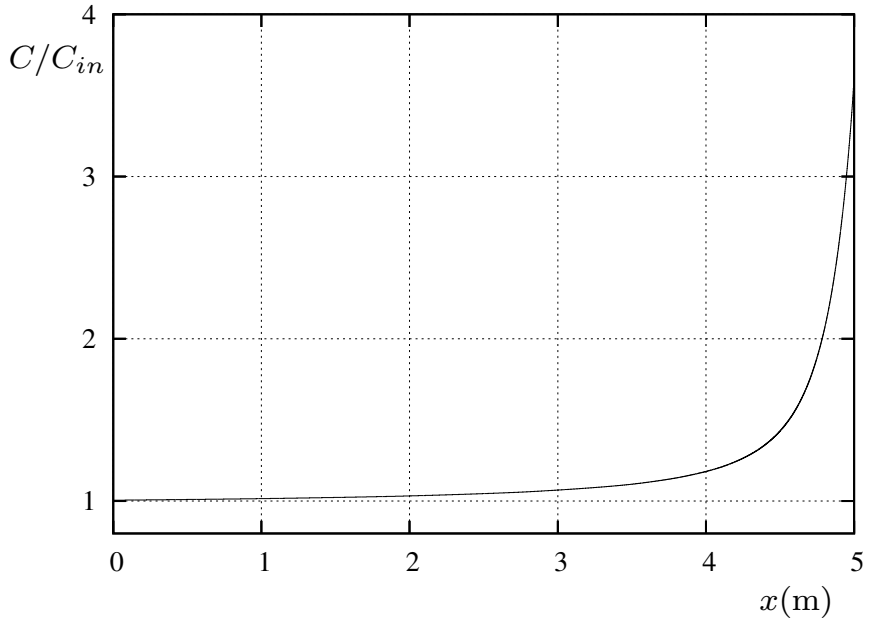

Figure 2: Relative concentration distributions of Kr along the source

Table 7: Calculated data for the mixture Kr-T_2

Throughput of T_2 [2]	2.913 mbar l/s
Throughput of Kr	$2.822 \times C_{in}$ mbar l/s
Column density of single gas [2]	5.00×10^{17} 1/cm^2
Column concentration of Kr	$1.06 \times C_{in}$

injection point.

Thus, for the mixture Kr-T_2 we cannot say that the separation phenomenon is negligible, but the nonuniform concentration along the source must be taken into account.

3 Simulation of turbo-molecular pump

3.1 Characteristics of the pump

In this section, results on numerical simulation of a turbo-molecular pump are reported. The specification of the pump purchased by the KATRIN program is MAG W 2800 CT manufactured by Leybold. The technical data of the pump provided by Leybold are given in Table 8. Some additional data obtained from drawings and pictures are given in Table 9.

In the present work a two-dimensional model of turbo-pump is employed. The scheme of the model is presented in Fig.3. We consider 11 rotors and 11 stators. The distance between the blades h and the blade width b are considered to be constant for all stages, while the blade inclination α_i varies from stage to stage. The blades of rotors move with a speed U. Our aim is to calculate the transmission probability W from high vacuum to fore vacuum, i.e. from the left hand side to the right one according to the scheme in Fig.3.

To realize the calculations besides of the data given in Tables 8 and 9 the following data are necessary: the distance between blades h, the rotor speed U and the blade inclinations α_i. The quantities h and U are not constant for one stage but they depend on the position, namely, on the radius. To calculate these quantities the mean square radius was used, i.e.

$$R_{ms} = \sqrt{(R_{ex}^2 + R_{in}^2)/2}, \tag{11}$$

where R_{ex} and R_{in} are external and internal radii of rotors, respectively. Then, the distance h was calculated as

$$h = \frac{2\pi R_{ms}}{N_b} = 0.0248 \text{ m}, \tag{12}$$

where $N_b = 24$ is the number of blades. The speed of rotors was also calculated on the basis of the mean square radius, i.e.

$$U = \omega R_{ms} = 286 \text{ m/s}, \tag{13}$$

Table 8: Data provided by Leybold

Quantity	Value
Pumping speed for N_2	2650 l/s
Pumping speed for Ar	2450 l/s
Pumping speed for He	2850 l/s
Pumping speed for H_2	2100 l/s
Compression for N_2	$> 10^8$
Rotor speed	28 800 rpm

Table 9: Information taken from drawings, pictures etc.

Quantity	Value
Number of rotors	N_r=11
Number of stators	N_s=11
External radius	R_{ex}=0.12 m
Internal radius	R_{in}=0.06 m
Number of blades	N_b=24
Blade width	b =0.025 cm

where ω is the rotation speed.

The blade inclinations α_i were not provided by Leybold. They were calculated to obtains the maximum pumping speed at the fixed values of h, b and U. As a result, the value of α_i was gradually decreased from 45° with the increment of 2° for the next pair of rotor-stator, i.e.

$$\alpha_i = 47^\circ - 2^\circ * i, \qquad 1 \leq i \leq 11. \tag{14}$$

3.2 Description of program

The program is based on the test particle Monte Carlo method. First, a particle is generated in accordance with the Maxwellian distribution function. At the same time, a position of the first rotor relatively the first stator is generated. Then, a motion of the particle in the rotor is simulated up to its exit. The particle position relatively the next stator is calculated on the basis of the time that the particle stayed in the rotor. These operations are repeated until the particle leaves the last stator or the first rotor. The transmission probability is calculated as

$$W = \frac{N_p}{N_g}, \tag{15}$$

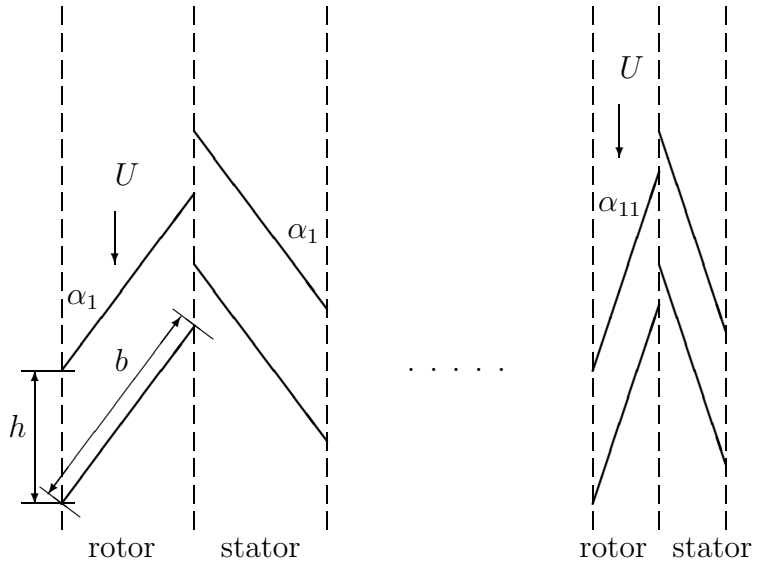

Figure 3: Scheme of 2D pump

where N_p is the number of particles that passed through the pump and N_g is the total number of generated particles.

A diffuse scattering of molecules on the blade surface was assumed. However, the diffuse-specular scattering is also considered in the numerical codes.

Since in practice the pump could be hotter than the pumping gas a possibility of such a difference was considered.

To test the numerical codes the results presented in Table II of Ref.[10] and Table 1 of Ref.[11] were reproduced.

3.3 Results of calculations

In every simulation 10^6 particles were tested to calculate the transmission probability W from high vacuum to fore vacuum. The pumping speed was calculated as

$$S = \frac{\sqrt{\pi}}{2}\frac{T}{273.15}(R_{ex}^2 - R_{in}^2)v_m W, \tag{16}$$

where T is the gas temperature, and v_m is the most probable molecular velocity

$$v_m = \left(\frac{2R_g T}{m}\right)^{1/2}, \tag{17}$$

Table 10: Results of simulation

gas	T K	T_p K	W	S l/s
N_2	293	293	0.509	2180
N_2	293	350	0.492	2109
Ar	293	293	0.566	2029
Ar	293	350	0.552	1977
He	293	293	0.231	2613
He	293	350	0.216	2447
H_2	293	293	0.165	2650
H_2	293	350	0.154	2473
T_2	27	300	0.402	104
T_2	30	300	0.397	120
T_2	50	300	0.363	237
T_2	80	300	0.334	441
T_2	100	300	0.321	592
T_2	120	300	0.312	756
T_2	140	300	0.305	932
T_2	160	300	0.299	1115
T_2	180	300	0.293	1305
T_2	200	300	0.289	1507

m is the molecular mass of the gas.

As is known a pump is heated during its functioning. However, no data about the pump temperature is available. To evaluate the influence of the pump temperature to the pumping speed some calculations were carried out for two values of the pump temperature, i.e. $T_p = 293$ K and 350 K.

The results of calculations are presented in Table 10. One can see that the influence of the pump temperature on the pumping speed is very weak. The present model provide a reasonable agreement with the data by Leybold for nitrogen argon and helium gases. However, there is a significant disagreement with the pumping speed for hydrogen.

The calculations for tritium were calculated assuming the pump temperature equal to 300K, while the gas temperature was varied from 27 K to 200 K. This is a supposed range of the temperature variation of the pumping gas. From Table 10 we conclude that the transmission probability gradually decreases from the value 0.402 to 0.289 by increasing the gas temperature.

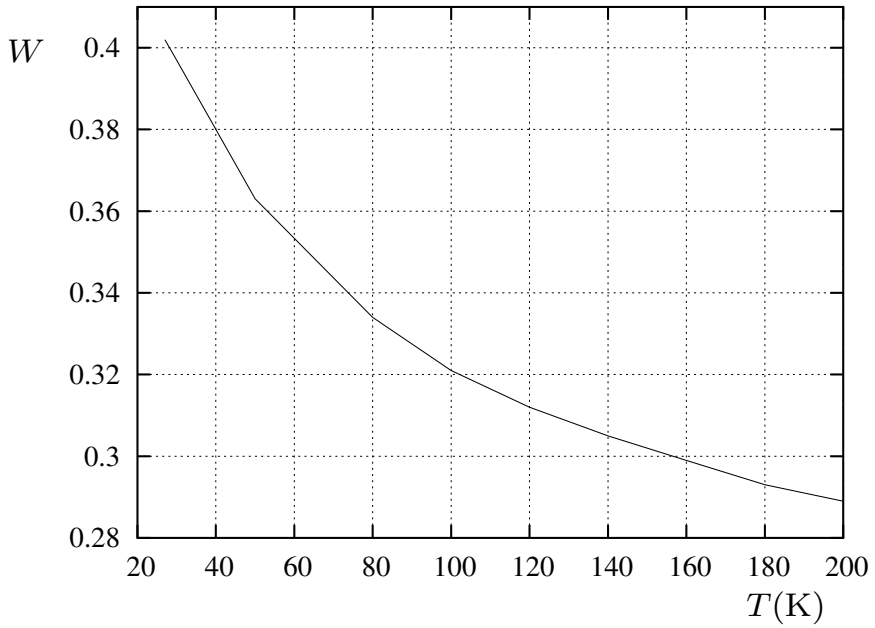

Figure 4: Transmission probability W vs temperature of gas T

To calculate the transmission probability from fore vacuum to high vacuum 10^9 particles were tested. None of them passed through the pump. So, we conclude that the compression ratio is larger than 10^8 that coincide with the data given by Leybold. However, it is impossible to calculate this quantity more precisely.

4 Concluding remarks

In the first part of the present work the separation phenomenon the source line was calculated. It was found that for the mixture H_2 - T_2 this phenomenon is weak, while for the mixture Kr - T_2 the separation phenomenon is significant.

In the second part of the work the transmission probability through a turbo-molecular pump for tritium was calculated for different temperature of tritium assuming the temperature of the pump equal to 300 K. If we assume that the temperature of tritium varies in the range from 27 K to 200 K then the transmission probability varies in the range from 0.289 to 0.402.

References

[1] F. Sharipov, "Numerical calculation of tririum flow through the KATRIN beam line," Technical report, Depto de Física, UFPR (2003) .

[2] F. Sharipov, "Calculations of tritium flow bewteen the buffer vessel up to the first vacuum sistem," Technical report, Depto de Física, UFPR (2004) .

[3] *Vacuum thechnology - Turbomolecular pumps - Measurements of performance characteristics*, International Organization for Standardization, 2003, ISO 5302:2002(E).

[4] F. Sharipov and D. Kalempa, "Gaseous mixture flow through a long tube at arbitrary Knudsen number," J. Vac. Sci. Technol. A **20,** 814–822 (2002).

[5] S. Naris, D. Valougeorgis, D. Kalempa, and F. Sharipov, "Gaseous mixture flow between two parallel plates in the whole range of the gas rarefaction," Physica A **336,** 294–318 (2004).

[6] S. Naris, D. Valougeorgis, F. Sharipov, and D. Kalempa, "Discrete velocity modelling of gaseous mixture flows in MEMS," Superlattices and Microstructures **35,** 629–643 (2004).

[7] S. Naris, D. Valougeorgis, D. Kalempa, and F. Sharipov, "Flow of gaseous mixtures through rectangular microchannels driven by pressure, temperature and concentration gradients," accepted in Phys. Fluids (2005).

[8] F. Sharipov and D. Kalempa, "Separation phenomena for gaseous mixture flowing through a long tube into vacuum," submitted to Phys. Fluids (2005).

[9] F. J. McCormack, "Construction of linearized kinetic models for gaseous mixture and molecular gases.," Phys. Fluids **16,** 2095–2105 (1973).

[10] S. Katsimichas, G. A. J. H, R. Lewington, and C. R. E. de Oliveira, "General geometry calculations of one-stage molecular flow transmission probabilities for turbomolecular pumps," J. Vac. Sci. Technol. A **13,** 2954–2961 (1995).

[11] T. N. Schneider, S. Katsimichas, C. R. E. de Oliveira, and A. J. H. Goddard, "Analysis of three-dimensional single stage and two- dimensional multistage models of flows in turbomolecular pumps," Vacuum **48,** 449–453 (1997).